

Analysis of soil organic matter accumulation in a millennium chronosequence using a spectral parameter

Chronosequence, consisting of a series of soil profiles, splices brief segments of soil evolution history¹ and translates spatial differences between soils into temporal differences to reveal the rate and direction of pedogenic changes². Many soil properties in a chronosequence exhibit time-dependent trends³. The accumulation of soil organic matter (SOM) is an important pedogenic process^{4,5}. SOM has a major influence on other properties such as cation exchange capacity and the contents of N, P and S⁶. SOM content in a profile is related to age of the soil⁷ and reveals the degree of soil development⁸. Traditional methods of determining SOM are slow, expensive and destructive, and thus do not satisfy the requirements for its rapid estimation or regional soil survey. On the other hand, soil spectroscopy has been widely used to estimate SOM due to its rapidity, convenience and cost-efficiency^{9–12}. Most researchers calibrated SOM using visible and near-infrared (VNIR) spectroscopy with partial least squares regression (PLSR) method^{13–15}. However, it is difficult to display and compare the changes in SOM in a chronosequence using the whole VNIR spectroscopy. In addition, a large number of multispectral airborne and space-borne sensors have relatively longer historical records than hyperspectral data. Thus, we need a simple parameter, which is derived from several bands to characterize SOM content. As we all know, the absorption of SOM decreases reflectance across the entire VNIR region, especially in the visible (VIS) region^{9,16}, and the strongest absorption by SOM occurs at 600 nm (ref. 17). High SOM content results in concave reflectance curves between 500 and 1300 nm, whereas low SOM content in convex reflectance curves¹⁸. Therefore, we can use the parameter ‘deviation of arch’ (DOA)¹⁹, which characterizes the concavity and convexity of spectral curves in the visible range, to display and analyse the changes in SOM between and within the profiles. Thus, the objectives of this study are to: (i) investigate SOM accumulation over a 1000-year period, (ii) evaluate the utility of DOA for analysing SOM accumulation and estimating SOM in a millennium chronosequence.

The study area is located in the coastal plain of Dongtai, northern Jiangsu Province, China (Figure 1). The coastal plain in this area developed from sediments transported mainly by the Yellow River and Yangtze River in the past 1000 years, affording an excellent object for the study of soil chronosequence. With northern subtropical monsoon climate, this region has a mean annual precipitation of 1042.3 mm and temperature of 15.0°C (ranging from –7.5°C to 35.9°C). These soils are cultivated with rice–wheat rotation systems after being reclaimed.

Soil ages were estimated based on the coastline changes²⁰, and seven soil profile samples were collected in the eastern area of the Fan Gong Dike (Figure 1, Table 1). The sampling depth intervals of each profile were 0–5, 5–10, 10–20, 20–30, 30–40, 40–60, 60–80 and 80–100 cm. The samples were ground in the laboratory after air-drying, and SOM was determined using the potassium dichromate method.

Air-dried soil samples, sieved with a 0.150 mm sieve, were used for spectral measurements. Soil reflectance spectra were measured in a dark room using a FieldSpec 3 portable spectrometer (Analytical Spectral Devices Inc, Boulder, Colorado, USA) with spectral resolution of 3 nm from 350 to 1000 nm and 10 nm from 1000 to 2500 nm. A 50 W halogen lamp positioned 30 cm (L, Figure 2) from the samples at a vertical angle of 15° (A, Figure 2) was used as a light source. The sensor was located vertically at a distance of 15 cm (H, Figure 2) from the soil samples using a probe with a 5° (B = 2.5°, Figure 2) viewing angle, producing a radius of 0.655 cm (R2, Figure 2) from the centre of the dish (R1 = 2.5 cm) (Figure 2). The soil sample in the container was rotated using an automatic rotating platform when the 20 spectral curves were collected. The reflectance spectrum of each sample was the mean of these 20 spectral curves. The

spectral curves were then smoothed using the Savitzky–Golay method (quadratic polynomial, 11 points) in Unscrambler 9.7 software (CAMO Inc, 2007).

The correlation coefficients between SOM and reflectance were more than 0.7 between 548 and 712 nm. The correlation was highest at 604 nm. DOA at 604 nm is defined as the difference between the linear fitted values from 548 to 712 nm and the reflectance at 604 nm of each spectral curve (Figure 3). DOA at 604 nm reflects the concave or convex feature of the spectral curve between 548 and 712 nm: DOA decreases with increase in SOM content.

SOM increased with soil age between profiles and decreased with depth within the profiles (Figure 4). The differentiation of the vertical distribution of SOM in the profiles increased with soil age, i.e. older soils presented more SOM differentiation in topsoil and subsoil. This observation suggested that the process of SOM accumulation was obvious in the surface soil within 30 cm depth due to the development of salt-tolerant plants and cultivation in the past 1000 years. SOM was uniform in the subsoil of 30–100 cm depth, except for the N4 profile, which suggested uniformity of the parent material.

The accumulation rates of SOM in different layers were different (Figure 5). SOM in the topsoil (0–5 cm) and 5–10 cm layer increased linearly with soil age in the first 900 years or so (Figure 5 *a* and *b*). However, the SOM in these two layers of N7 was dramatically lower than N6, which suggested that there was some unknown reason. SOM in the layers of 10–20 cm and 20–30 cm showed logarithmic relationships with soil age and accumulated rapidly in the first 400 years or so (Figure 5 *c* and *d*).

SOM content showed a negative correlation with DOA, and the correlation coefficient was –0.78 (significant level of 0.01). Therefore, DOA showed inverse trends versus SOM between and within

Table 1. Age of soil profiles in Dongtai chronosequence

Number	N1	N2	N3	N4	N5	N6	N7
Soil age (yr)	150	250	400	500	750	900	1000

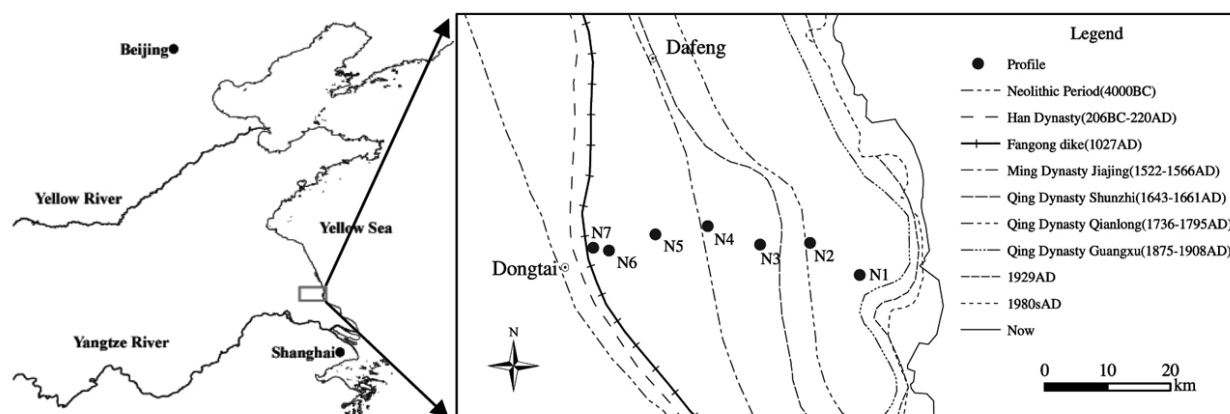


Figure 1. Location of the study area and sampling sites.

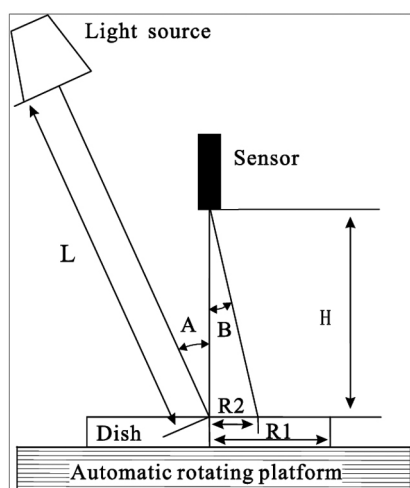


Figure 2. Optical set-up of the spectrometer.

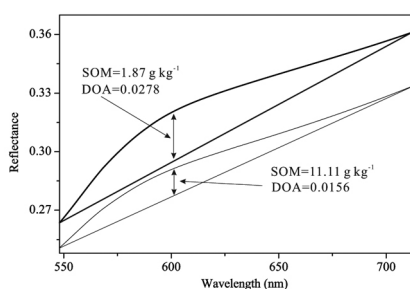


Figure 3. Deviation of arch changes with soil organic matter.

the profiles (Figures 4 and 6), and it can be used to display the changing trends of SOM this chronosequence. However, DOA values of N4 displayed a clear difference from those of the other profiles due to the high SOM content in the layer of 20–60 cm (Figure 4).

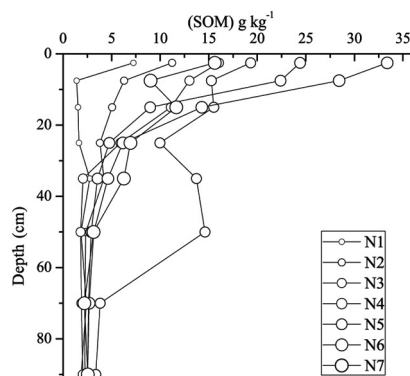


Figure 4. Depth distribution of soil organic matter.

Linear and logarithmic functions were used to fit the scatters of SOM and DOA, and good results were obtained ($R^2 = 0.5970$ and $R^2 = 0.6669$ respectively) (Figure 7). These results suggested that SOM could be estimated using this simple spectral parameter, DOA, and logarithmic model gave better results.

This study examined the characteristics of SOM accumulation process over a period of 1000 years and evaluated utility of the simple parameter, DOA, for analysing SOM accumulation. In the past decades, numerous soil chronosequence studies have found that SOM content increases with age, i.e. SOM content is higher in older soils^{5,21} and may reach a steady state when soils reach a dynamic equilibrium with their environment. However, the accumulation rate of SOM changes and the relationship between SOM and age was different in many studies. Egli *et al.*²² and He and Tang²³

found that SOM accumulated at very high rates within the first 200 years or less in the soil of proglacial areas. VandenBygaart and Protz⁸ concluded that the relationship between SOM and soil age was logarithmic. However, Lilienfein *et al.*²⁴ reported that soil carbon increased linearly during approximately the first 600 years, after which the accumulation rates decreased. In the present study, SOM in the 0–10 cm layer increased linearly with soil age except the profile of 1000 years, which suggested that SOM in this layer would continue to increase in the future. The relationship between SOM in the 10–30 cm and soil age was logarithmic, which suggested that SOM in this layer would not increase dramatically. The rate of soil development, including SOM accumulation, was mainly affected by climate²⁵ and cultivation²⁶. In this study, paddy cultivation, such as manuring for cropping, additions form roots and straw remaining contributes to the accumulation of SOM of surface soil and low decomposition rate under anaerobic condition favours the accumulation of SOM²⁷.

DOA regression for SOM has been rarely used in recent studies since its initial proposal by Xu and Dai¹⁹. The possible reasons are the advances in computation and instrumentation and developments in multivariate statistics, which make it possible to solve the problem of collinearity among independent variables. For example, the method of partial least squares regression can extract the information from the whole range of 350–2500 nm and give a better regression result^{28,29}. However, DOA includes the most important spectral

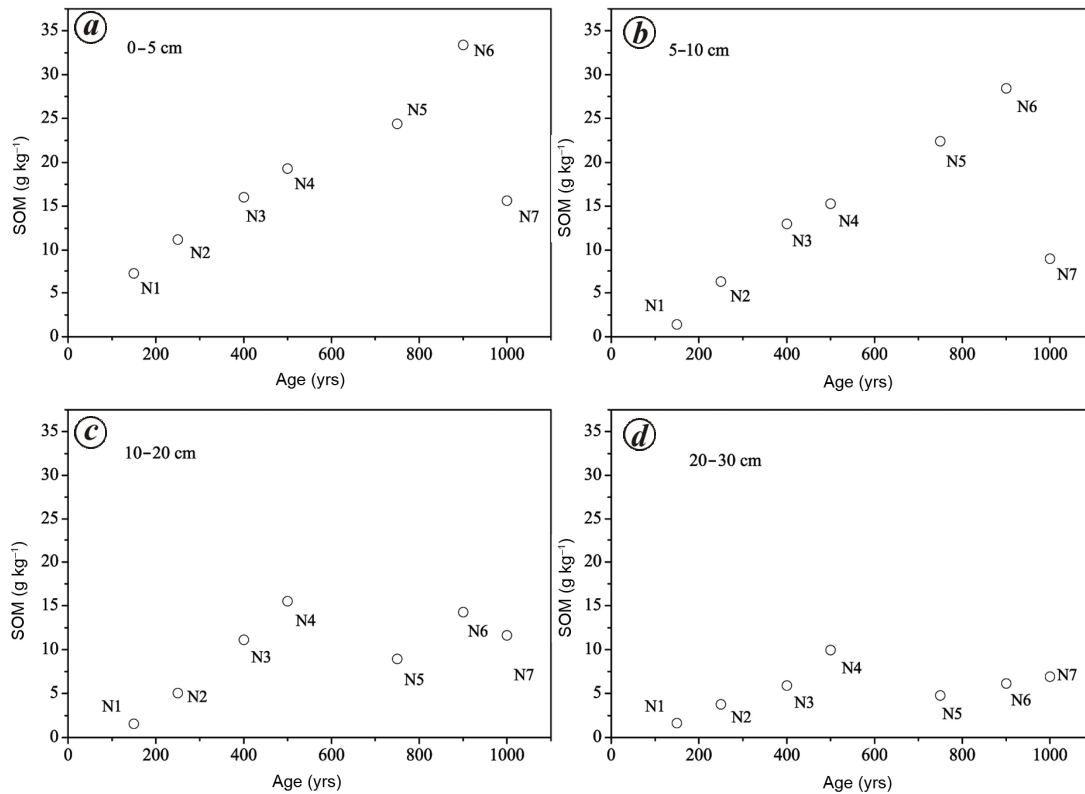


Figure 5. Accumulation of SOM in different layers within 30 cm depth.

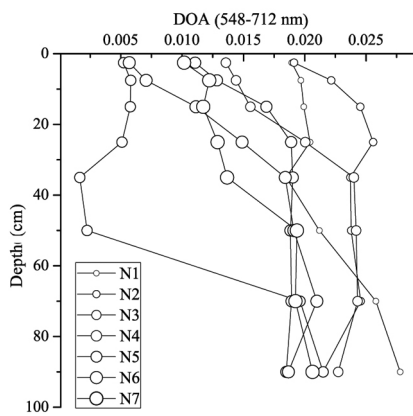


Figure 6. Depth distribution of deviation of arch.

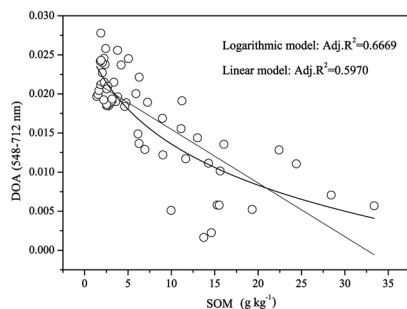


Figure 7. Scatters and regression lines of soil organic matter and deviation of arch.

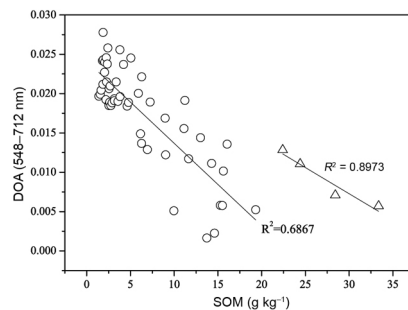


Figure 8. Linear regression lines of two datasets with 20 g kg⁻¹ as cut-off.

information regarding SOM and reflects the changes in SOM, although it requires only three bands. It is a useful parameter for rapid analysis of SOM accumulation process and SOM estimation. The relationship between DOA and SOM varies due to the high spatial heterogeneity and variation in SOM. For example, the power function yielded the optimal results in the study by Xu and Dai¹⁹. In the present study, linear model gave better results when the samples were divided into two datasets according to SOM content, with 20 g kg⁻¹ as the cut-off^{30,31} (Figure 8) which suggested that variation

in SOM content had an important effect on its quantitative estimation.

In this millennium chronosequence, SOM increased with soil age, and SOM accumulation occurred mainly within the first 30 cm depth. SOM content in the topsoils (0–10 cm) increased linearly, while in the 10–30 cm layer it increased logarithmically with soil age during the observed time-span. We can also conclude that DOA is a useful parameter for analysing the pedogenic process of SOM accumulation in a millennium chronosequence and estimating SOM content. However, further studies are needed for cases in which SOM content in other areas is markedly different.

1. Jenny, H., *The Soil Resource: Origin and Behaviour*, Springer, New York, 1980, pp. 207–245.
2. Huggett, R. J., *Catena*, 1998, **32**, 155–172.
3. Chen, L. M., Zhang, G. L. and Effland, W. R., *Soil Sci. Soc. Am. J.*, 2011, **75**, 1807–1820.
4. Tsai, C. C., Tsai, H., Hseu, Z. Y. and Chen, Z. S., *Catena*, 2007, **71**, 394–405.
5. Vilmundardóttir, O. K., Gísladóttir, G. and Lal, R., *Geomorphology*, 2015, **228**, 124–133.

6. Certini, G. and Scalenghe, R., *Soils: Basic Concepts and Future Challenges*, Cambridge University Press, New York, 2012, pp. 45–55.
7. Wissing, L., Kolbl, A., Vogelsang, V., Fu, J. R., Cao, Z. H. and Kogel-Knabner, I., *Catena*, 2011, **87**, 376–385.
8. VandenBygaart, A. J. and Protz, R., *Can. J. Soil Sci.*, 1995, **75**, 63–72.
9. Ben-Dor, E., *Adv. Agron.*, 2002, **75**, 173–243.
10. Nanni, M. R. and Demattè, J. A. M., *Soil Sci. Soc. Am. J.*, 2006, **70**, 393–407.
11. Jarmer, T., Vohland, M., Hillenthal, H. and Schnug, E., *Pedosphere*, 2008, **18**, 163–170.
12. Xie, X. L., Pan, X. Z. and Sun, B., *Pedosphere*, 2012, **22**, 351–366.
13. Viscarra Rossel, R. A. and Behrens, T., *Geoderma*, 2010, **158**, 46–54.
14. Shen, Z. Q., Shan, Y. J., Peng, L. and Jiang, Y. G., *Pedosphere*, 2013, **23**, 305–311.
15. St Luce, M., Ziadi, N., Zebbarth, B. J., Grant, C. A., Tremblay, G. F. and Gregorich, E. G., *Geoderma*, 2014, **232–234**, 449–458.
16. Viscarra Rossel, R. A., Walvoort, D. J. J., McBratney, A. B., Janik, L. J. and Skjemstad, J. O., *Geoderma*, 2006, **131**, 59–75.
17. Brown, D. J., Shepherd, K. D., Walsh, M. G., Mays, M. D. and Reinsch, T. G., *Geoderma*, 2006, **132**, 273–290.
18. Huete, A. R. and Escadafal, R., *Remote Sensing Environ.*, 1991, **35**, 149–159.
19. Xu, B. B. and Dai, C. D., *Chin. Sci. Bull.*, 1980, **6**, 282–284.
20. Zhang, R. S., *Acta Geogr. Sin.*, 1984, **39**, 173–184.
21. Lichter, J., *Geoderma*, 1998, **85**, 255–282.
22. Egli, M., Mavris, C., Mirabella, A. and Giaccai, D., *Catena*, 2010, **82**, 61–69.
23. He, L. and Tang, Y., *Catena*, 2008, **72**, 259–269.
24. Lillienfein, J., Qualls, R. G., Uselman, S. M. and Bridgham, S. D., *Geoderma*, 2003, **116**, 249–264.
25. Bockheim, J. G., *Geoderma*, 1980, **24**, 71–85.
26. Fu, Q. L., Ding, N. F., Liu, C., Lin, Y. C. and Guo, B., *Geoderma*, 2014, **230–231**, 50–57.
27. Huang, L. M., Thompson, A., Zhang, G. L., Chen, L. M., Han, G. Z. and Gong, Z. T., *Geoderma*, 2015, **237–238**, 199–210.
28. Vasques, G. M., Grunwald, S. and Sickman, J. O., *Soil Sci. Soc. Am. J.*, 2009, **73**, 176–184.
29. Ladoni, M., Bahrami, H. A., Alavipanah, S. K. and Norouzi, A. A., *Precis. Agric.*, 2010, **11**, 82–89.
30. Baumgardner, M. F., Kristof, S., Johannsen, C. J. and Zachary, A., *Proc. Indiana Acad. Sci.*, 1970, **79**, 413–422.
31. Galvao, L. S. and Vitorello, I., *Int. J. Remote Sensing*, 1998, **19**, 1969–1979.

ACKNOWLEDGEMENTS. This study was supported by the National Natural Science Foundation of China (No. 41201215 and No. 41301505). The map of soil type used in sampling was provided by Data Sharing Infrastructure of Earth System Science (www.geodata.cn). We thank Jingchen Zheng for help during the field work. We also thank Changqiao Hong, Junfeng Xiong, Minmin Huang, Yuting Tao, Yongwei Gan, Jiangjie Jia and Cheng Lv for sample processing and spectral measurements.

Received 25 June 2015; revised accepted 13 March 2018

GUANGHUI ZHENG*

CAIXIA JIAO

GANG SHANG

FENFANG LIN

*School of Geographical Sciences,
Nanjing University of Information
Science and Technology,
Nanjing, China*

*For correspondence.

e-mail: zgh@nuist.edu.cn

Emergence of multidrug-resistant *Raoultella ornithinolytica* associated with Indian major carp

Raoultella ornithinolytica is a Gram-negative, non-motile bacillus belonging to the family Enterobacteriaceae and has been associated with hospital-acquired clinical cases. The pathogenic potential of *R. ornithinolytica* isolates in human disease has become increasingly important¹. The well-known factors involved in pathogenicity of *R. ornithinolytica* are its ability to adhere to human tissue, to convert histidine to histamine and to form biofilms in urinary catheters and other surgical equipment. The clinical presentations of infections include bacteraemia^{2,3}, enteric fever⁴, diabetic foot⁵, urinary tract infection, biliary tract infection, community and hospital-acquired pneumonia, pleural effusion, osteomyelitis, meningitis, cerebral abscess, pericarditis, conjunctivitis, otitis and skin infections⁶. A high rate of hospital-acquired infections has been reported in patients with immunodeficiency and

those who have undergone invasive procedures, e.g. mechanical ventilation, urinary catheters and post-urethral trauma¹. This bacterium, along with closely related species *R. planticola*, has been shown to be the causative agent of histamine toxicity from fish (also known as scombroid syndrome), but is frequently misidentified as *Klebsiella pneumoniae*. Histamine toxicity results from the expression of histidine decarboxylase, which enables the bacterium to convert histidine, and produces symptoms that include flushing, pruritus, headache and abdominal cramping⁷. Over the past decade, *R. ornithinolytica* has emerged as an infrequent, but important causative agent of human infections⁸. To the best of our knowledge, few cases of *R. ornithinolytica* human infection have been reported worldwide, linking this pathogen to bacteraemia, sepsis, soft tissue and other infections⁹. The bacterium

has also been isolated from human digestive organs¹.

Indian major carp (IMC), commonly known as rohu, is one of the most preferred aquaculture fish species among the carps in India and commands a higher market price. However, with the increase in aquaculture production of rohu, occurrence of diseases proves to be significant setback for successful aquaculture by spoilage during cultivation, preservation and trading problems caused by pathogenic bacteria. The most common bacterial pathogens in IMC found in this region are *Aeromonas hydrophila*, *A. liquefaciens*, *A. sorbia*, *A. veronii*, *Edwardsiella tarda*, *Providencia vermicola*, *Acinetobacter baumannii*, *Pseudomonas fluorescence*, *Shigella* sp. and *Chondrococcus columnaris*. *A. hydrophila* accounts for the most common pathogen in IMC and has zoonotic significance¹⁰. The aquatic environment harbours